Original Article	*Curr. Appl. Sci.*, **2026**, *4*(1): 66-73 DOI:10.22034/cas.2026.574826.1060	Current Applied Sciences

Surface Plasmon Excitation in a Spherical Nanocavity: The Hydrodynamical Drude Model

Moslem Mir

Department of Physics, Faculty of Science, University of Zabol, Zabol, 98615-538, Iran

Corresponding author's e-mail: *moslem.mir@uoz.ac.ir*

Article Information

Received: 10 February 2026
Revised: 17 February 2026
Accepted: 19 February 2026
Published online: 24 February 2026

Keywords

Localized surface plasmons
Spatial nonlocality effects
Spherical nanocavity
Surface plasmon

Abstract

We theoretically study nonlocal effects in surface plasmon excitations in a spherical dielectric nanocavity embedded in a metallic host within the framework of the hydrodynamic Drude model. An analytical expression for the surface plasmon resonance frequencies is derived, enabling a transparent interpretation of size-dependent and material-dependent plasmonic behavior beyond the local approximation. Nonlocality is shown to modify the plasmonic response, leading to a blueshift of the resonance frequencies as the nanocavity radius decreases. We further demonstrate that the background dielectric constant associated with the metal ion core plays an essential role in the excitation process. For nanocavities with dielectric constants smaller than that of the metallic background, the surface plasmon resonances shift to higher frequencies, while a redshift occurs when the cavity dielectric constant exceeds the background value. In addition, increasing the nanocavity dielectric constant enhances the influence of nonlocal effects on surface plasmon excitations. These parameters offer valuable guidance for the design of subwavelength plasmonic structures.

1. Introduction

Collective electronic excitations in metals, known as plasmons, are a fundamental component of their electromagnetic response. These excitations can occur either as bulk plasmons, corresponding to charge-density oscillations within the metal volume, or as surface plasmons, which are localized at metal–dielectric interfaces of nanostructures [1]. Owing to their confinement and dispersion properties, surface plasmons can exhibit effective resonance frequencies that differ significantly from those of bulk modes, particularly in complex or nanoscale geometries. This characteristic has been widely exploited in the development of ultrafast plasmonic electronic components and high-sensitivity sensing platforms [2].

The behavior of plasmonic excitations is strongly governed by geometry. Nanostructures such as metallic nanospheres, spherical nanoshells, and dielectric nanocavities have attracted considerable attention, as their plasmonic resonances can be tuned over a broad spectral range extending from the terahertz to the visible region [3]. These high-frequency modes make such nanostructures essential building blocks for emerging applications in subwavelength photonic circuitry and active plasmonic devices [4, 5].

Although classical electrodynamics based on local dielectric functions provides an adequate description for structures with dimensions well above the nanometer scale [6, 7], it becomes insufficient as characteristic sizes approach a few nanometers. In this regime, nonlocal effects—originating from the finite compressibility of the electron gas, spatial dispersion, and electron–electron interactions—become increasingly important [8]. To incorporate these effects without the computational cost of first-principles methods, semi-analytical frameworks such as the hydrodynamic Drude model (HDM) [9, 10] and the Generalized Nonlocal Optical Response (GNOR) [11, 12] are widely employed.

In this work, we investigate the role of spatial nonlocality in surface plasmon excitations of a spherical dielectric nanocavity embedded in a metallic host within the framework of the HDM. An analytical expression for the surface plasmon resonance frequencies is derived, demonstrating a pronounced size-dependent blueshift induced by nonlocal effects as the nanocavity radius is reduced. We further show that the interplay between the dielectric constant of the nanocavity and the background permittivity associated with the metal ion core plays a central role in determining the excitation characteristics. Specifically, a lower cavity permittivity leads to an increase in the resonance frequency, whereas a higher permittivity results in a redshift. Importantly, we find that nonlocal frequency shifts are most strongly enhanced for high-index dielectric cavities, offering valuable guidance for the design and optimization of subwavelength plasmonic structures.

2. Materials and Methods

2.1 *Hydrodynamical Drude model*

In metals, conduction electrons form a degenerate electron gas that undergoes frequent scattering from the ionic lattice and impurities. Within the hydrodynamic description, the electron gas is treated as a semi-classical charged fluid moving in a uniform positive background. The collective dynamics of the electrons are described using the HDM, which incorporates both convective motion and damping effects. In this approach, the electron dynamics are obtained by self-consistently solving the following set of equations, including [13]:

Hydrodynamic equation,

$$m_e n\left(\frac{\partial \vec{v}}{\partial t} + (\vec{v}.\vec{\nabla})\vec{v}\right) = -\vec{\nabla}P(n) - ne\vec{E} - m_e n\,\Gamma\,\vec{v}, \quad (1)$$

Continuity equation,

$$\frac{\partial n}{\partial t} + \vec{\nabla}.(n\vec{v}) = 0, \quad (2)$$

and Poisson equation

$$\vec{\nabla}.\vec{E} = -\frac{e(n - n_0)}{\varepsilon_0 \varepsilon_B}. \quad (3)$$

Here, m_e denotes the electron mass, $n(\vec{r}, t)$ is the electron number density, and n_0 is the ion (equilibrium electron) density. The terms $\vec{v}(\vec{r}, t), P(n)$, Γ, ε_0, and ε_B represent the electron velocity, the pressure due to the

Pauli exclusion principle, the damping constant, the permittivity of free space, and the relative permittivity of background ions, respectively. Within the HDM framework, the non-local spatial effect is captured by $\vec{\nabla}P(n) = m_e\beta^2\vec{\nabla}n$, with $\beta^2 = (3/5)v_F^2$, (v_F being the Fermi velocity). Under the quasi-static approximation, the electric field is defined as $\vec{E} = -\vec{\nabla}\phi$, which is then inserted into the Poisson equation.

To analyze the system's dynamics, the set of coupled equations (1) through (3) is linearized by assuming small-amplitude perturbations about the equilibrium. By adopting a harmonic time-dependence, the perturbations for velocity, density, and potential are defined as follows:

$$\begin{aligned} n(\vec{r},t) &= n_0 + \delta n^{(1)}(\vec{r})\exp(-i\Omega t), \\ \vec{v}(\vec{r},t) &= \vec{v}^{(1)}(\vec{r})\exp(-i\Omega t), \\ \phi(\vec{r},t) &= \phi^{(1)}(\vec{r})\exp(-i\Omega t), \end{aligned} \qquad (4)$$

with $\Omega = \omega + i\omega_I$, where ω and ω_I are the real and imaginary components of the frequency. Substituting Eqs. (4) into Eqs. (1)–(3) and keeping only the linear terms yields the following system of equations:

$$m_e n_0\left(-i\Omega\,\vec{v}^{(1)}\right) = -m_e\beta^2\vec{\nabla}\delta n^{(1)} + n_0 e\vec{\nabla}\phi^{(1)} - m_e n_0\,\Gamma\vec{v}^{(1)}, \quad (5)$$

$$\left(-i\Omega\,\delta n^{(1)}\right) + n_0\vec{\nabla}.\,\vec{v}^{(1)} = 0, \qquad (6)$$

$$\nabla^2\phi^{(1)} = \frac{e\delta n^{(1)}}{\varepsilon_0\varepsilon_B}. \qquad (7)$$

Taking the divergence of both sides of Eq. (5) and then substituting Eqs. (6) and (7) into the result, we obtain

$$(\beta^2\nabla^2 - \bar{\omega}_p^2 + \omega^2 - \omega_I^2 + \Gamma\omega_I)\delta n^{(1)} + i\,(2\omega\omega_I + \Gamma\omega) = 0. \qquad (8)$$

The imaginary part of Eq. (8) yields $\omega_I = -\Gamma/2$. Substituting it in the real part of Eq. (8), we obtain the final differential equation governing the electron density:

$$(\nabla^2 - k^2)\delta n^{(1)}(r) = 0, \qquad (9)$$

with $k^2 = \left(\bar{\omega}_p^2 - \omega^2 - \Gamma^2/4\right)/\beta^2$, where $\bar{\omega}_p = \sqrt{n_0 e^2/m_e\varepsilon_0\varepsilon_B}$, is the plasma frequency of metallic region. By solving Eq. (9), the surface and bulk plasmon frequencies are obtained for the regime $\omega > \sqrt{\bar{\omega}_p^2 - \Gamma^2/4}$ and $\omega < \sqrt{\bar{\omega}_p^2 - \Gamma^2/4}$, respectively.

2.2 *Surface plasmon frequency of a nanocavity*

Consider a metallic medium with ε_B containing a dielectric nanocavity characterized by a relative permittivity ε_d (see Figure 1). Solving Eq. (9) yields the following expression for the electron-density excitation at the metal surface:

$$\delta n^{(1)}(r,\theta,\varphi) = \begin{cases} \sum_{l,m} A_{l,m}\,k_l(kr)\,y_{l,m}(\theta,\varphi)\ , & r \geq R, \\ 0, & r < R, \end{cases} \qquad (10)$$

where $k_l(kr)$ is modified spherical Bessel function of the second kind and $y_{l,m}(\theta,\phi)$ are the spherical harmonic functions. The electron density inside the nanocavity is zero.

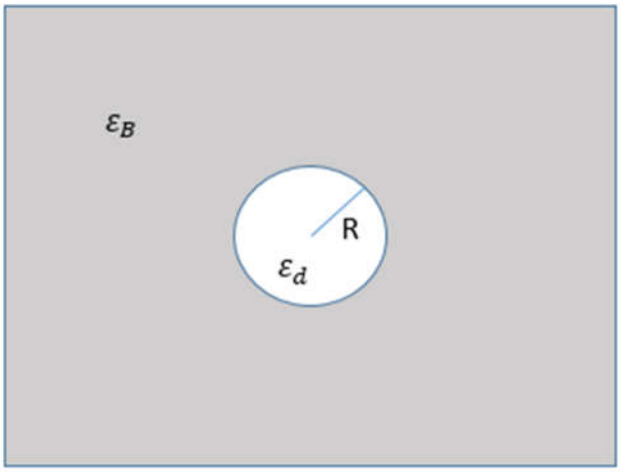

Figure 1. Schematic illustration of a nanocavity with radius R and dielectric permittivity ε_d embedded within a metallic region with background permittivity ε_B

Subsequently, we derive the electric potential for both the metallic region (the region outside the dielectric nanocavity) and the nanocavity region. To obtain the potential outside the nanocavity, the electron density, $\delta n^{(1)}$, from Eq. (7), is first substituted into Eq. (9), and we find

$$(\nabla^2 - k^2)\nabla^2\phi_{out}(r,\theta,\varphi) = 0. \qquad (11)$$

Solving the above equation yields the following expression for the potential outside the nanocavity:

$$\phi_{out}(r,\theta,\varphi) = \sum_{l,m}\left(B_{l,m}k_l(kr) + C_{l,m}\, r^{-(l+1)}\right)\, y_{l,m}(\theta,\varphi). \qquad (12)$$

Because there is no net charge within the nanocavity, the potential satisfies Laplace's equation, which we solve to obtain

$$\phi_{in}(r,\theta,\varphi) = \sum_{l,m} D_{l,m}\, r^l\, y_{l,m}(\theta,\varphi). \qquad (13)$$

To derive the nanocavity's plasmonic modes, the potential coefficients within the metallic region are determined in terms of the corresponding electron density coefficients. We then employ the boundary condition: The radial component of the electron density becomes zero at the surface of the nanocavity.

To determine the potential coefficients for the regions inside and outside the nanocavity, we first apply the continuity conditions for the electric potential and the displacement vector at the nanocavity surface.

$$\phi_{in}(r,\theta,\varphi)|_{r=R} = \phi_{out}(r,\theta,\varphi)|_{r=R},$$

$$\varepsilon_d \frac{\partial\phi_{in}(r,\theta,\varphi)}{\partial r}\bigg|_{r=R} = \varepsilon_B \frac{\partial\phi_{out}(r,\theta,\varphi)}{\partial r}\bigg|_{r=R}.$$

Applying the above boundary conditions, the potential outside the nanocavity is given by the following relations:

$$\phi_{out}(r,\theta,\varphi) = \sum_{l,m} B_{l,m}\left[k_l(kr) - Q_l(kR,\bar{\varepsilon})\left(\frac{R}{r}\right)^{l+1}\right] y_{l,m}(\theta,\varphi), \qquad (14)$$

where

$$Q_l(kR,\bar{\varepsilon}) = \frac{kR}{2l+1}\left[k_{l+1}(kR) + \frac{(1-\bar{\varepsilon})l}{(l+1)+l\bar{\varepsilon}}k_{l-1}(kR)\right],$$

in which $\bar{\varepsilon} = \varepsilon_d/\varepsilon_B$. The potential inside the nanocavity is given by

$$\phi_{in}(r,\theta,\varphi,t) = \sum_{l,m} B_{l,m}\, P_l(kR,\bar{\varepsilon})(\frac{r}{R})^l\, y_{l,m}(\theta,\varphi), \qquad (15)$$

where

$$P_l(kR,\bar{\varepsilon}) = -\frac{kR}{l+1+\bar{\varepsilon}\, l} k_{l-1}(kR).$$

To determine the surface plasmon frequencies of the nanocavity, we apply the condition that the radial current density vanishes at the nanocavity surface.

$$J_r|_{r=R} = 0 \rightarrow v_r|_{r=R} = 0.$$

Substituting the velocity from Eq. (5) and applying the vanishing radial boundary condition, the following expression is obtained:

$$\frac{n_0 e}{m_e}\frac{\partial \phi_{out}(r,\theta,\varphi)}{\partial r}\bigg|_{r=R} = \beta^2 \frac{\partial \delta n_{out}(r,\theta,\varphi)}{\partial r}\bigg|_{r=R} \qquad (16)$$

By substituting the potential from Eq. (14) and the charge density from Eq. (10) into Eq. (16) and using the relation $k^2 B_{l,m} = (e/\varepsilon_0\, \varepsilon_B) A_{l,m}$,the following expression for the nanocavity surface plasmons is obtained:

$$\left(\bar{\omega}_p^2 - \beta^2\, k^2 + \frac{(l+1)(\bar{\varepsilon}-1)}{l+1+l\bar{\varepsilon}}\bar{\omega}_p^2\right) l\, k_{l-1}(kR) \; = (l+1)\, \beta^2\, k^2\, k_{l+1}(kR). \qquad (17)$$

If $\varepsilon_d = \varepsilon_B$ ($\bar{\varepsilon} = 1$), the following expression results:

$$\left(\bar{\omega}_p^2 - \beta^2\, k^2\right) l\, k_{l-1}(kR) = (l+1)\, \beta^2\, k^2\, k_{l+1}(kR). \qquad (18)$$

In the local limit ($\beta \rightarrow 0$), Eq. (18) reduces to the following relation:

$$\omega = \sqrt{\frac{(l+1)\bar{\omega}_p^2}{l+1+l\bar{\varepsilon}} - \frac{\Gamma^2}{4}}. \qquad (19)$$

In the absence of the scattering, Eq. (19) gives

$$\omega = \bar{\omega}_p \sqrt{\frac{(l+1)}{l+1+l\bar{\varepsilon}}}, \qquad (20)$$

which for $l = 1$ and $\varepsilon_d = \varepsilon_B = 1$ is [1],

$$\omega = \omega_p \sqrt{\frac{2}{3}}.$$

3. Results and Discussion

Using a silver (Ag) metallic region with parameters $\omega_p = 13.52 \times 10^{15}\, rad/s$, $\Gamma = 5.88 \times 10^{13}\, 1/s$, $\varepsilon_B = 5$, and $v_F = 1.39 \times 10^6 m/s$, the relative permittivity (dielectric constant) of the nanocavity is $\varepsilon_d = 5$ [14]. In the following, we consider the dipole approximation, setting $l = 1$ in Eq. (17). Figure 2 illustrates the normalized dipole surface plasmon frequencies (ω/ω_p) as a function of the nanoparticle radius (R). The results demonstrate that spatial nonlocality leads to a significant blueshift in resonance frequencies at smaller radii. The local response approximation is also plotted for comparison, showing a size-independent behavior.

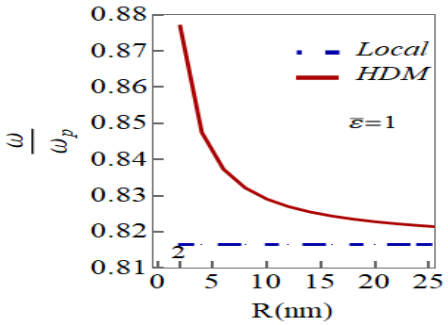

Figure 2. The dimensionless dipole surface plasmon frequency vs. the radius of a nanocavity in the Ag metallic region for $\bar{\varepsilon} = 1$ ($\bar{\varepsilon} = \varepsilon_d/\varepsilon_B$). The system parameters are $\omega_p = 13.52 \times 10^{15}\ rad/s$, $\Gamma = 5.88 \times 10^{13}\ 1/s$, $\varepsilon_B = 5$, $v_F = 1.39 \times 10^6 m/s$ and $\varepsilon_d = 5$

In Figure 3, the normalized surface plasmon frequency is plotted as a function of radius R for three dielectric configurations. The results indicate that the resonance frequency is sensitive to the dielectric contrast: When $\bar{\varepsilon} > 1$ ($\varepsilon_d > \varepsilon_B$), the frequencies shift toward lower values (redshift), whereas for $\bar{\varepsilon} < 1$ ($\varepsilon_d < \varepsilon_B$), the frequencies are blue-shifted relative to the baseline case of $\bar{\varepsilon} = 1$ ($\varepsilon_d = \varepsilon_B$). Notably, all configurations exhibit a nonlocal frequency increase as the nanoparticle radius decreases.

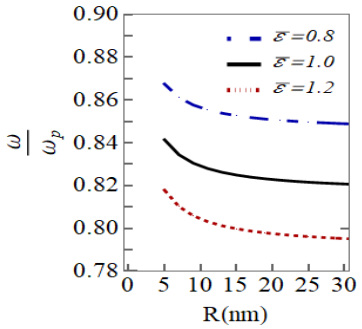

Figure 3. The dimensionless dipole surface plasmon frequency vs. the radius of a nanocavity in the Ag metallic region for different values of $\bar{\varepsilon}\ (= \varepsilon_d/\varepsilon_B)$. The other system parameters are $\omega_p = 13.52 \times 10^{15}\ rad/s$, $\Gamma = 5.88 \times 10^{13}\ 1/s$, and $v_F = 1.39 \times 10^6 m/s$.

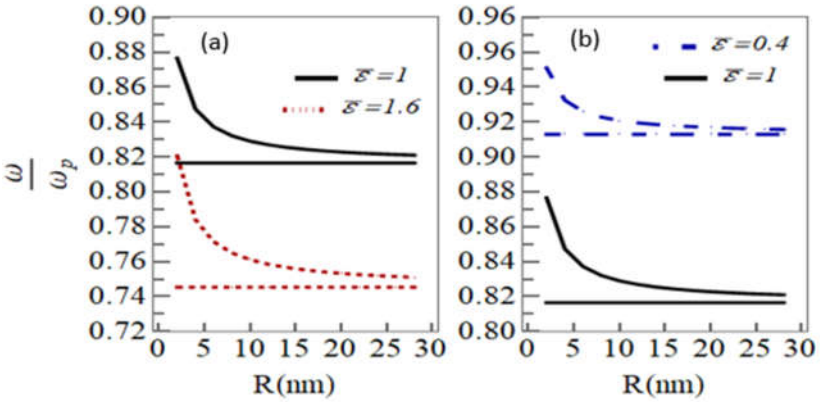

Figure 4. Nonlocal and local dimensionless dipole surface plasmon frequency vs. the radius of a nanocavity in the Ag metallic region for (a) $\bar{\varepsilon} = 1.6$ and (b) $\bar{\varepsilon} = 0.4$. In both panels, the dimensionless nonlocal and local surface plasmon frequencies for $\bar{\varepsilon} = 1$ are plotted for comparison. The system parameters are $\omega_p = 13.52 \times 10^{15}\ rad/s$, $\Gamma = 5.88 \times 10^{13}\ 1/s$, $v_F = 1.39 \times 10^6 m/s$, and $\bar{\varepsilon} = \varepsilon_d/\varepsilon_B$

Figure 4 illustrates the influence of the nanocavity dielectric constant (ε_d) on spatial nonlocality. The results demonstrate that the nonlocal frequency shift is significantly enhanced when the dielectric constant of the nanocavity is increased relative to the background medium. By comparing the local (horizontal lines) and nonlocal results, it is evident that the blueshift caused by nonlocality is more substantial for larger values of ε_d. Specifically, the deviation from the local limit at small radii is greater in panel (a) for $\bar{\varepsilon} = 1.6$ ($\varepsilon_d = 1.6\ \varepsilon_B$) than in panel (b) for $\bar{\varepsilon} = 0.4$ ($\varepsilon_d = 0.4\ \varepsilon_B$).

4. Conclusion

In conclusion, we have developed a nonlocal theoretical description of surface plasmon excitations in spherical metallic nanocavities. By deriving an analytical resonance condition, we have quantified the frequency shifts induced by spatial nonlocality on the nanoscale. Our results demonstrate that the background dielectric constant of the metal plays an essential role in determining the direction of the plasmonic frequency shift: the resonance is blue-shifted or red-shifted depending on whether the cavity permittivity is smaller or larger than the background value, respectively. Furthermore, we show that nonlocal effects are significantly amplified in nanocavities with high dielectric permittivity. These findings highlight the importance of accounting for both spatial nonlocality and the dielectric environment when designing nanocavity-based plasmonic devices, including sensors and nanoscale optical components.

Acknowledgment

The authors acknowledge the use of an AI-based language tool to assist with editing and improving the clarity and readability of the manuscript. The scientific content, analysis, and conclusions are entirely the responsibility of the authors.

Conflicts of Interest

The author declares that there are no conflicts of interest regarding this article.

References

1. Maier SA. Plasmonics: Fundamentals and Applications. New York: Springer. 2007.
2. Gonçalves MR, Minassian H, Melikyan A. Plasmonic Resonators: Fundamental Properties and Applications. *J. Phys. D: Appl. Phys.* 2020, 53, 443002.
3. Mcoyi MP, Mpofu KT, Sekhwama M, Mthunzi-Kufa P. Developments in Localized Surface Plasmon Resonance. *Plasmonics* 2025, 20, 5481--5520.
4. Zhang C, Ding T. Active Plasmonic Nanodevices: From Basic Principles to Emerging Applications. *Responsive Mater.* 2024, 2, e20240024.
5. Davis TJ, Gómez DE, Roberts A. Plasmonic circuits for manipulating optical information. *Nanophotonics* 2017, 6, 543-559.
6. Park SY, Stroud D. Surface-plasmon dispersion relations in chains of metallic nanoparticles: An exact quasistatic calculation. *Phys. Rev. B* 2004, 69, 125418.
7. Weber WH, Ford W. Propagation of optical excitations by dipolar interactions in metal nanoparticle chains. *Phys. Rev. B* 2004, 70, 125429.

8. Ding T, Tserkezis C, Mystilidis C, Vandenbosch GAE, Zheng X. Quantum Mechanics in Plasmonic Nanocavities: from Theory to Applications. *Adv. Physics Res.* 2025, 4, 2400144.
9. García de Abajo FJ. Nonlocal Effects in the Plasmons of Strongly Interacting Nanoparticles, Dimers, and Waveguides. *J. Phys. Chem. C* 2008, 112, 17983-17987.
10. Barberán N, Bausells J. Plasmon Excitation in Metallic Spheres. *Phys. Rev. B* 1985, 31, 6354-6362.
11. Mortensen NA, Raza S, Wubs M, Søndergaard T, Bozhevolnyi SIA. Generalized Non-Local Optical Response Theory for Plasmonic Nanostructures. *Nat. Commun*. 2012, 5, 3809.
12. Wubs M, Mortensen NA. Nonlocal response in plasmonic nanostructures. *In* Quantum plasmonics. Cham: Springer International Publishing. 2016, pp. 279-302.
13. Mir M. Spatial nonlocality effect on the surface plasmon propagation in plasmonic nanospheres waveguide. *J. Phys.: Condens. Matter* 2023, 35, 205301.
14. Yang HU, D'Archange J, Sundheimer ML, Tucker F, Boreman GD, Raschke MB. Optical dielectric function of silver, *Phys. Rev. B* 2015, 91, 235137.

How to cite this article: Mir M. Surface Plasmon Excitation in a Spherical Nanocavity: The Hydrodynamical Drude Model. *Curr. Appl. Sci.*, 2026, 4(1):66-73. https://doi.org/10.22034/cas.2026.574826.1060